UIOWA-92-10

Fermilab Library
0 1160 0010612 4

UIOWA-92-10
May 1992

The Total Neutrino Cross Section at Very High Energies*

MARY HALL RENO

Department of Physics and Astronomy,
University of Iowa, Iowa City, Iowa 52242, USA

AUG 21 1992

ABSTRACT

Issues related to the small x behavior of the parton distribution functions are reviewed. Their implications for the total neutrino cross section are presented.

ROUTE TO
LOCATION
NAME
RETURN TO FERMILIBRARY

* To appear in the Proceedings for the Workshop on High Energy Neutrino Astrophysics, University of Hawaii, Honolulu, Hawaii, March 23-26, 1992.

THE TOTAL NEUTRINO CROSS SECTION AT VERY HIGH ENERGY

M. H. RENO
Department of Physics and Astronomy, University of Iowa
Iowa City, Iowa 52242, USA

ABSTRACT

Issues related to the small x behavior of the parton distribution functions are reviewed, Their implications for the total neutrino cross section are presented.

1. Introduction

There are a variety of theoretical models for ultrahigh energy neutrino sources of astrophysical and cosmological origin.[1] The total neutrino-nucleon cross section as a function of incident neutrino energy is an essential input into any calculation of expected event rates for neutrino to muon conversion in large underground detectors. The low energy cross section is well known. Indeed, much of our knowledge of the nucleon structure functions comes from neutrino-nucleon and electron-nucleon deep inelastic scattering (DIS) experiments from laboratory neutrino beams.[2–3] With predictions of non-trivial fluxes from astrophysical and cosmic sources of neutrinos with energies up to $\sim 10^{10}$ GeV, an understanding of the theoretical issues in the calculation at very high energies is essential. Presented here is the standard calculation of the total neutrino cross section and a review of the theoretical status of the small-x behavior of the parton distribution functions.[4] Theoretical parameterizations of the small-x behavior have implications for the total cross section, as much as a factor of two at the highest energies.

The standard computation of the neutrino-nucleon cross section in the QCD improved parton model requires the parton level cross sections convoluted with the parton distribution functions. All of the results presented are for isoscalar nucleon targets (N). This assumption has little effect at neutrino energies larger than $\sim 10^5$ GeV, as above this energy, the sea quark contributions dominate. For definiteness, we refer to an incident ν_μ, so in the charged current process, the final state includes a muon. We take the muon to be massless, so the results apply to electron neutrino scattering as well. The lowest order Feynman graphs for the charged current cross section involve neutrino-quark and neutrino-antiquark interactions via a spacelike $W^{\pm}$ boson. The parton level result is convoluted with

the quark and antiquark distribution functions to give

$$\sigma(\nu_\mu N \to \mu X) = \int_0^1 \mathrm{d}\,x \int_0^1 \mathrm{d}\,y \, \frac{2G_F^2 M E_\nu}{\pi} \left[\frac{M_W^2}{Q^2 + M_W^2}\right]^2 \cdot$$

$$\cdot[xq(x,Q^2) + x(1-y)^2\bar{q}(x,Q^2)],$$

for a nucleon with mass M. Here, $q^2 = (p_\nu - p_\mu)^2 = -Q^2$ is the square of the four-momentum transfer, $y = (E_\nu - E_\mu)/E_\nu$ in the lab frame, and $x = Q^2/(2ME_\nu y)$. The parton distributions $q(x,Q^2)$ and $\bar{q}(x,Q^2)$ contributing to νN charged current scattering are

$$q = d + s + b$$
$$\bar{q} = \bar{u} + \bar{c} + \bar{t}\,.$$

Given the current lower bound on the top quark mass of 91 GeV/c^2,[5] top sea contributions are not included in the numerical calculation. The neutral current cross section has a similar form:

$$\sigma(\nu_\mu N \to \nu X) = \int_0^1 \mathrm{d}\,x \int_0^1 \mathrm{d}\,y \, \frac{G_F^2 M E_\nu}{2\pi} \left[\frac{M_Z^2}{Q^2 + M_Z^2}\right]^2 \cdot$$

$$\cdot[xL_q^2\big(q(x,Q^2) + (1-y)^2\bar{q}(x,Q^2)\big) + xR_q^2\big((1-y)^2 q(x,Q^2) + \bar{q}(x,Q^2)\big)]$$

where $L_q = \tau_3 - 2Q_q \sin^2\theta_W$ and $R_q = -2Q_q \sin^2\theta_W$. Here, $\tau_3 = \pm 1$, Q_q is the quark electric charge and θ_W is the weak mixing angle. All quarks and antiquarks contribute to the neutral current scattering.

At low energies and low Q^2, theory predicts that $\sigma \sim E_\nu$. At low values of Q^2, the distribution functions are nearly scale independent and the weak gauge boson propagator is dominated by the boson mass, M_W or M_Z. The average value of y is $\sim 1/2$, so $x \sim Q^2/(ME_\nu)$. As E_ν rises, there are several effects that change the cross section's growth with energy. First, at fixed Q^2, with increasing E_ν, x decreases. The valence quark distributions decrease with decreasing x, however, the sea quark distributions are larger at small x, and increase with larger Q^2. On the other hand, larger Q^2 means a suppression of the cross section from the boson propagator. The net effect is a growth of the cross section with neutrino energy which is less than linear.

At the highest energies, the growth in Q^2 is effectively cut off by the boson propagator. Taking $Q^2 \sim M_W^2$ and $y \sim 1/2$,

$$x \sim \frac{M_W^2}{ME_\nu}.$$

At $E_\nu = 10^{10}$ GeV, this amounts to $x \sim 10^{-6}$, so at the highest neutrino energies, the parton distribution functions are probed at very small x. Experimental measurements of the parton distribution functions, however, do not extend into the small-x regime. At present, deep inelastic scattering experiments measure parton distributions for $x \gtrsim 0.01$ and 5 GeV$^2 \lesssim Q^2 \lesssim$ 250 GeV^2.[3] To leading order, the gluon does not contribute in DIS, however, $xG(x, Q^2)$ integrated over x is constrained by the momentum sum rule. Other experiments such as hadron production of real or virtual photons further constrain the form of the gluon distribution.[6] At HERA,[7] where an electron beam collides with a proton beam with center of mass energy $\sqrt{s} = 314$ GeV, experiments will be able to probe down to $x \sim 5 \cdot 10^{-5}$ for $Q^2 \geq 5$ GeV^2. Until HERA data are analysed, parameterizations of the parton distribution functions below $x = 10^{-2}$ are largely unconstrained.

The Altarelli-Parisi evolution equations dictate the parton distributions' evolution with $\ln Q^2$. The standard procedure is to use measured distributions at $Q_0^2 = 5$ GeV^2, then evolve via the Altarelli-Parisi equations for $Q > Q_0$. Because the evolution accounts for parton splitting such as $g \to q\bar{q}$, the gluon distribution feeds into the sea distributions at higher values of Q. A comparison of the measured and theoretical distributions at several scales serves as a constraint on the parameterizat'ons. Nevertheless, there are a variety of theoretical treatments of the parton distribution functions at small x, all consistent in the measured regime. In practice, the $\ln Q^2$ evolution is done numerically and computer programs using a variety of parameterizations extrapolate to $x_{\min} = 10^{-5}$ or 10^{-4}. These distributions are characterized by their gluon parameterizations, choice of the QCD scale Λ_{QCD} and the order in the QCD coupling α_s (one-loop or two-loop) to which the evolution equations are computed. We shall concentrate here on the Kwiecinski *et al.*[8] two-loop evolved distribution functions (KMRS) and set 2 of the Eichten *et al.*[9] one-loop distributions (EHLQ). There are a variety of other parameterizations that generally fall within the extreme predictions of two KMRS parameterizations.[10] For the KMRS results, the $\overline{\text{MS}}$ four flavor Λ_{QCD} is 190 MeV, and for EHLQ, $\Lambda_{\text{QCD}} = 290$ MeV. The KMRS distributions sweep out a range of possibities for the small-x behavior.

2. Small x extrapolation

Since experimental measurements of the parton distributions do not go below $x \sim 10^{-2}$, the small-x extrapolations of the parton distribution functions are guided by theoretical considerations. One approach is to consider the small-x limit of the Altarelli-Parisi evolution equations. In the double leading-logarithm approximation (DLA),[11] where only leading $\ln(Q^2/\Lambda^2)$ and $\ln(1/x)$ are kept, the Altarelli-Parisi equations can be solved analytically. This yields for the small x sea and gluon distributions, denoted by $f(x, Q^2)$, a functional form:

$$xf(x, Q^2) = C(Q^2)\Big(\frac{2(\xi - \xi_0)}{\rho}\Big)^{1/2} \exp\Big[\big(2\rho(\xi - \xi_0)\big)^{1/2}\Big]$$

where $\rho = (8N/b_0)\ln(1/x)$, $\xi(Q^2) = \ln\ln(Q^2/\Lambda^2)$ and $\xi_0 = \xi(Q_0^2)$. Here $N = 3$ is the number of colors and $b_0 = (11N - 2n_f)/3$ where $n_f = 5$ is the number of flavors. $C(Q^2)$ is fixed by matching the DLA form to the numerical values from the full Altarelli-Parisi evolution at $x = x_{\min}$ It is this small-x parameterization that was used in earlier computations of the total neutrino cross section for $x < 10^{-4}$.[12]

At very small x, one would like to keep all terms that are leading in $\ln(1/x)$, even subleading $\ln(Q^2/\Lambda^2)$ terms. This can be done via the Balitzkij-Lipatov equation[13] which can be approximately solved to give, in the small-x limit,

$$xf(x, Q^2) \sim x^{-p}$$

where p is calculated[13] to be approximately 1/2. This corresponds to a bare pomeron intercept $\alpha_P^0 \simeq 3/2$ in the Regge limit.[4] Two of the KMRS parameterizations at small x and $Q_0^2 = 5$ GeV^2 are therefore

$$\begin{aligned} B0: \quad xG(x, Q_0^2) &= c_1 \\ B-: \quad xG(x, Q_0^2) &= c_2 x^{-1/2} \end{aligned}$$

according to the traditional form at $Q^2 = Q_0^2$ (B0) or the approximate solution to the Balitzkij-Lipatov equation (B-). The evolution and numerical stablity of the KMRS distributions are valid over the range $10^{-5} < x < 1$ and 5 GeV^2 $< Q^2 < 1.31 \cdot 10^6$ GeV^2.[8] The actual solution to the problem should lie somewhere between these two extremes because of an additional complication, namely, the

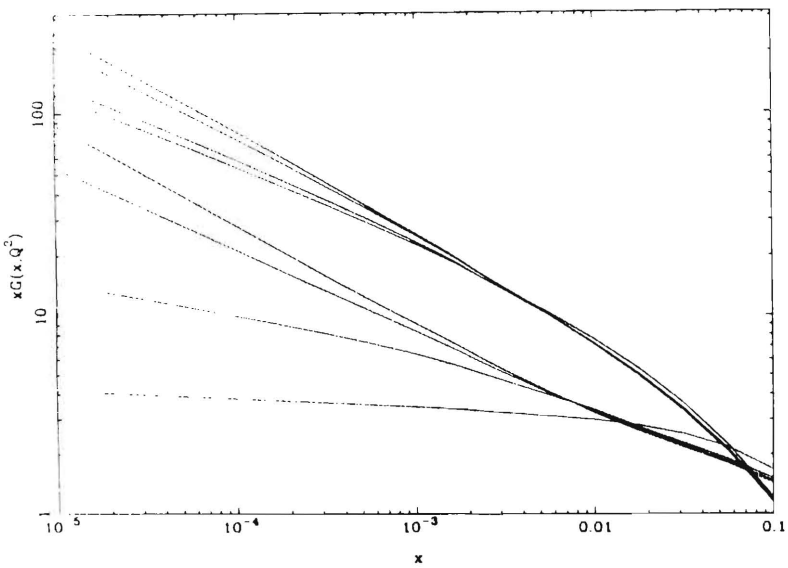

Fig. 1. The gluon distribution function $xG(x,Q^2)$ as a function of x for $Q^2 = 5, 5000$ GeV^2 (lower and upper sets of four lines) for the KMRS[8] distributions B-, B-5 B-2 and B0. The B- distribution is the highest of each set of four, the B0 distribution is the lowest.

so-called "shadowing corrections" to the evolution equations.[14] In the small-x limit,

$$\frac{\partial(xG(x,Q^2))}{\partial \ln Q^2} \simeq \frac{3\alpha_s(Q^2)}{\pi} \int_x^1 \frac{dy}{y}(yG(y,Q^2))$$
$$- \frac{9\pi}{16}\frac{1}{\pi R^2}\left(\frac{3\alpha_s(Q^2)}{Q}\right)^2 \int_x^1 \frac{dy}{y}(yG(y,Q^2))^2$$

where R roughly characterizes the size of the nucleon. In fact, there are numerous contributions to recombination including gluons from two different quarks in the nucleon and gluons from the same quark. If it is the former, then $R \sim 5$ GeV^{-1}, otherwise $R \sim 2$ GeV^{-1}, corresponding to the KMRS B-5 and B-2 sets.

The form of the shadowing correction is such that at low Q^2, where $\alpha_s(Q^2)/Q^2$ is large, the change to the $1/\sqrt{x}$ distributions are significant, whereas at higher Q^2, the net effect is to slightly modify the power law. The KMRS parton distributions incorporate the low Q^2 corrections into the starting form of the gluon and sea distributions as well as include the shadowing term in the evolution of the distributions. Shown in Fig. 1 is x versus $xG(x,Q^2)$ for $Q^2 = 5$ GeV^2 and

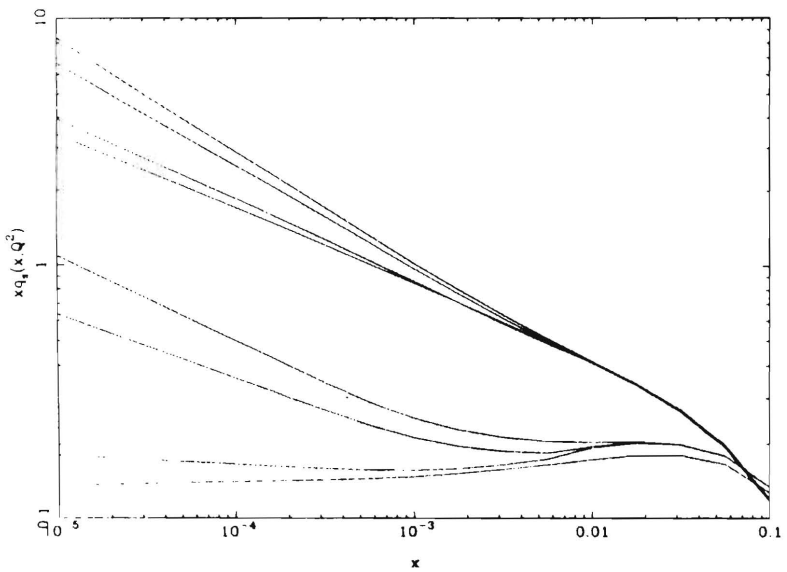

Fig. 2. The up sea quark distribution function $xq_s(x, Q^2)$ as a function of x for $Q^2 = 5, 5000$ GeV^2 (lower and upper sets of four lines) for the KMRS[8] distributions B-, B-5 B-2 and B0. The B- distribution is the highest of each set of four, the B0 distribution is the lowest.

$Q^2 = 5000$ GeV^2 for the B-, B-5, B-2 and B0 distributions, in order of decreasing size. Fig. 2 shows the up sea quark distribution for the same parameterizations and values of Q^2. For $x \lesssim 10^{-3}$, the net effect of the shadowing, for large Q^2, is to modify the power p in

$$xf(x, Q^2) \sim x^{-p}$$

from $p = 1/2$ to $p < 1/2$.

In order to evaluate the neutrino cross section up to energies of order 10^{10} GeV, we need to extrapolate beyond the nominal range of validity of the KMRS distributions. This is done here by extrapolating the B-, B-5 and B-2 $xG(x, Q^2)$ and the sea distributions below $x = 10^{-5}$ using the power p at $x = 10^{-5}$ and $Q = M_W$. This assumes that at $Q^2 \sim M_W^2$, there is little effect due to shadowing except to establish p. From Figs. 1 and 2, it appears that the power is essentially constant for $10^{-5} \leq x \leq 10^{-3}$ for each of the distributions. The power p for each of the gluon distributions changes little for Q between 50-200 GeV, so this should not be a bad approximation. Also checked was the fact that the shadowing correction for $Q = M_W$ and $x \geq 10^{-7}$ is still a small correction to the Altarelli-

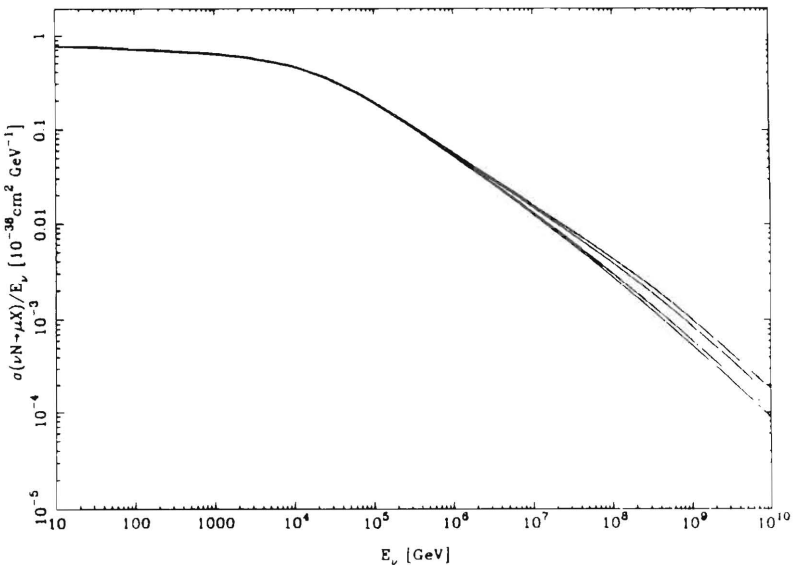

Fig. 3. The charged current cross section for $\nu N \to \mu X$ divided by neutrino energy for B0, B-2, B-5 and B- distributions.

Parisi evolution, namely,

$$\frac{9\pi^2}{16}\frac{1}{\pi R^2}\frac{3\alpha_s(Q^2)}{Q^2}xG(x(Q^2) \ll 1 \ .$$

At $x = 10^{-7}$, this quantity is approximately 0.05. Thus, the extrapolation below $x = 10^{-5}$ relevant for $\sigma(\nu N)$ up to $E_\nu = 10^{10}$ GeV should be reliable. The B0 distribution is extrapolated using the DLA extension to small x.

3. Numerical implications

The implications of the different parton distributions are seen in Fig. 3. In order of increasing size are shown $\sigma(\nu N \to \mu X)/E_\nu$ vs. E_ν for B0, B-2, B-5 and B- distributions in units of 10^{-38} cm^2/GeV. Table 1 gives a numerical assessment of the sizes of the charged current results computed with several choices of distribution functions, relative to the B0 calculation. As discussed above, the B0 and B- cross sections should be taken as the extreme limits of the theoretical predictions. The B-2 and B-5 theoretical results should be closer to the actual values. The cross sections computed with the EHLQ Set 2 distributions lie closest to the B-5 results. Finally, in Fig. 4, we show the B- and B0 computations of the charged current and charged plus neutral current cross sections as functions of energy. The numbers for the total charged plus neutral cross sections are found in Table 2.

4. Final Comments

$\sigma(\nu N \to \mu X)/E_\nu$ $[10^{-38}\mathrm{cm}^2/\mathrm{GeV}]$			
E_ν [GeV]	B0	B0:B-2:B-5:B-	EHLQ
10^1	0.76	1:1:1:1	0.70
10^2	0.70	1:1:1:1	0.63
10^3	0.62	1:1:1:1	0.57
10^4	0.45	1:1:1:1	0.42
10^5	0.19	1:1:1:1	0.19
10^6	$0.52 \cdot 10^{-1}$	1:1:1.1:1.1	$0.55 \cdot 10^{-1}$
10^7	$0.12 \cdot 10^{-1}$	1:1:1.2:1.3	$0.14 \cdot 10^{-1}$
10^8	$0.27 \cdot 10^{-2}$	1:1.1:1.4:1.6	$0.33 \cdot 10^{-2}$
10^9	$0.54 \cdot 10^{-3}$	1:1.1:1.6:1.9	$0.73 \cdot 10^{-3}$
10^{10}	$0.91 \cdot 10^{-4}$	1:1.1:1.7:2	$0.15 \cdot 10^{-3}$

Table 1. The charged current cross section divided by neutrino energy using the B0 distributions, the ratio of the charged current cross sections using the B0, B-2, B-5 and B- distributions and the EHLQ Set 2 prediction for the cross section.

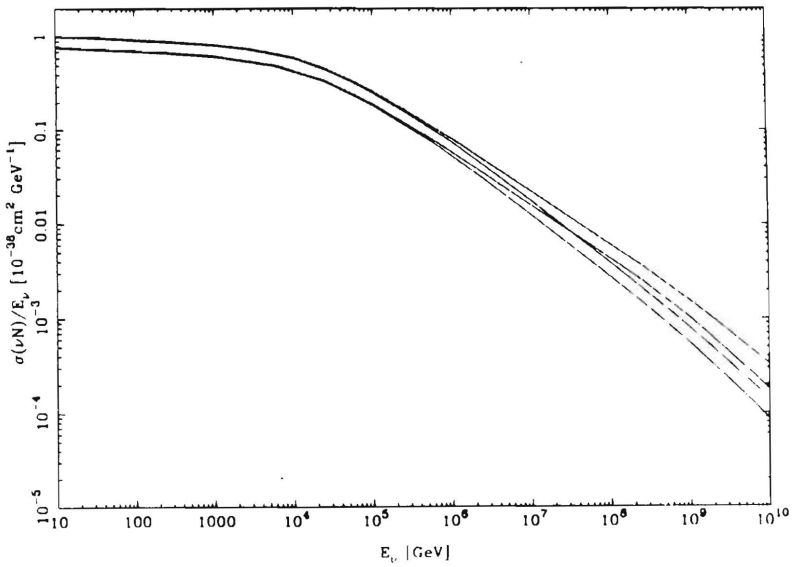

Fig. 4. The charged current and total (charged plus neutral current) cross sections for νN interactions, divided by neutrino energy for the B0 and B- distributions.

The results presented here are computed with the leading order parton level cross section. The inclusion of the $O(\alpha_s)$ perturbative correction to the hard scattering cross section changes the results by at most $\pm$ 10% , depending on the neutrino energy.[15] At low energies, the corrections are negative; at high energies, they are positive. While we have concentrated on the KMRS distributions here,

$\sigma_{\rm tot}(\nu N)/E_\nu$ [10^{-38}cm^2/GeV]			
E_ν [GeV]	B0	B-	EHLQ
10^1	1.00	1.02	0.91
10^2	0.91	0.94	0.82
10^3	0.81	0.83	0.74
10^4	0.60	0.61	0.56
10^5	0.25	0.26	0.26
10^6	$0.72{\cdot}10^{-1}$	$0.79{\cdot}10^{-1}$	$0.75 \cdot 10^{-1}$
10^7	$0.17{\cdot}10^{-1}$	$0.22{\cdot}10^{-1}$	$0.19 \cdot 10^{-1}$
10^8	$0.38{\cdot}10^{-2}$	$0.60{\cdot}10^{-2}$	$0.45 \cdot 10^{-2}$
10^9	$0.78{\cdot}10^{-3}$	$0.15{\cdot}10^{-2}$	$0.10 \cdot 10^{-2}$
10^{10}	$0.14{\cdot}10^{-3}$	$0.33{\cdot}10^{-3}$	$0.21 \cdot 10^{-3}$

Table 2. The sum of charged plus neutral current cross sections divided by neutrino energy using the B0, B- and EHLQ Set 2 distributions.

here, there are a variety of other distributions available. The Morfin-Tung[10] distributions also cover a broad range of possibilities, and the numerical evaluation of the QCD evolution of the distributions is not cut off at a minimum x value. Taking the distributions that give the largest neutrino cross section gives a charged current cross section almost a factor of ten larger than the B0 prediction at $E_\nu = 10^{10}$ GeV. Shadowing corrections were not applied to this calculation, so this cross section should be taken as an overestimate. Given the form of the remaining Morfin-Tung parton distributions at small x and $Q = M_W$,[4] one expects that the cross sections computed with these distributions should lie within the KMRS extreme limits at large E_ν.

5. Acknowledgements

I would like to thank the Department of Physics and Astronomy at the University of Hawaii for their hospitality. This work was supported in part by U.S. National Science Foundation Grant No. PHY-9104773.

6. References

1. See, *e.g.*, F. W. Stecker, C. Done, M. H. Salamon and P. Sommers, *Phys. Rev. Lett.* **66** (1991) 2697; C. T. Hill and D. N. Schramm, *Phys. Rev.* **D31** (1985) 564; J. H MacGibbon and R. H. Brandenberger, *Nucl. Phys.* **B331** (1990) 153; C. T. Hill, D. N. Schramm and T. P. Walker, *Phys. Rev.* **D36** (1987) 1007.

2. P. Auchincloss *et al.* (CCFR Collaboration), *Z. Phys.* **C48** (1990) 411; J.

Allaby *et al.* (CHARM Collaboration), *Z. Phys.* **C38** (1988) 403; P. Berge *et al.* (CDHS Collaboration), *Z. Phys.* **C35** (1987) 443.

3. M. Arneodo *et al.* (EMC) *Nucl. Phys.* **B333** (1990) 1; A. C. Benvenuti *et al.* (BCDMS Collaboration) *Phys. Lett.* **B223** (1989) 485; J. P. Berge *et al.*(CDHSW Collaboration) *Z. Phys.* **C49** (1991) 187; P. Z. Quintas *et al.* (CCFR Collaboration), Nevis Laboratory preprint NEVIS-1457 (August, 1991).
4. A more extensive review may be found in, *e.g.*, B. Badelek, K. Charchula, M. Krawczyk and J. Kwiecinski, "Small x Physics," DESY preprint DESY 91-124 (October 1991).
5. F. Abe *et al.* (CDF Collaboration), *Phys. Rev. Lett.* **68** (1992) 447.
6. A. S. Ito *et al.*, *Phys. Rev.* **D23** (1981) 604; C. N. Brown *et al.*, *Phys. Rev. Lett.* **63** (1988) 371.
7. See, *e.g.*, R. D. Peccei, ed., "Proceedings of the HERA Workshop," Hamburg, 1987.
8. J. Kwiecinski, A. D. Martin, W. J. Stirling and R. G. Roberts, *Phys. Rev.* **D42** (1990) 3645.
9. E. Eichten, I. Hinchliffe, K. Lane and C. Quigg, *Rev. Mod. Phys.* **56** (1984) 579, Errat.: **58** (1986) 1065.
10. Other parameterizations include: J. G. Morfin and W. K. Tung, *Z. Phys.* **C52** (1991) 13; P. N. Harriman, A. D. Martin, W. J. Stirling and R. G. Roberts, *Phys. Rev.* **D42** (1990) 798; M. Diemoz *et al.*, *Z. Phys.* **C39** (1988) 21; M. Glück, E. Reya and A. Vogt, *Z. Phys.* **C48** (1990) 471; D. Duke and J. Owens, *Phys. Rev.* **D30** (1984) 49; M. Glück *et al.*, *Z. Phys.* **C13** (1982) 119.
11. L. V. Gribov, E. M. Levin and M. G. Ryskin, *Phys. Rep.* **100** (1983) 1.
12. D. W. McKay and J. P. Ralston, *Phys. Lett.* **167B** (1986) 103; C. Quigg, M. H. Reno and T. P. Walker, *Phys. Rev. Lett.* **57** (1986) 774; M. H. Reno and C. Quigg, *Phys. Rev.* **D37** (1988) 657; T. K. Gaisser and A. F. Grillo, *Phys. Rev.* **D36** (1987) 2752.
13. Ya. Ya. Balitzkij and L. N. Lipatov, *Sov. J. Nucl. Phys.* **28** (1978) 822; J. B. Bronzan and R. L. Sugar, *Phys. Rev.* **D17** (1978) 585.
14. A. H. Mueller and J. Qiu, *Nucl. Phys.* **B268** (1986) 427; L. V. Gribov, E. M. Levin and M. G. Ryskin, *Nucl. Phys.* **B188** (1981) 155; *Sov. Phys. JETP* **53** (1981) 113.

15. G. Altarelli, R. K. Ellis and G. Martinelli, *Nucl. Phys.* **B157** (1979) 461; *Nucl. Phys.* **B143** (1978) 521; Errat. **B146** (1978) 544.